RM L58D17

NACA

RESEARCH MEMORANDUM

SOME EFFECTS OF MASS RATIO ON THE TRANSONIC FLUTTER CHARACTERISTICS OF UNTAPERED 45° SWEPTBACK WINGS OF ASPECT RATIOS 2 AND 3.5

By H. Neale Kelly

Langley Aeronautical Laboratory
Langley Field, Va.

NATIONAL ADVISORY COMMITTEE FOR AERONAUTICS

WASHINGTON

June 24, 1958

NATIONAL ADVISORY COMMITTEE FOR AERONAUTICS

RESEARCH MEMORANDUM

SOME EFFECTS OF MASS RATIO ON THE TRANSONIC FLUTTER CHARACTERISTICS OF UNTAPERED 45° SWEPTBACK WINGS OF ASPECT RATIOS 2 AND 3.5

By H. Neale Kelly

SUMMARY

A study has been made of the effects of mass ratio on the transonic flutter characteristics of untapered 45° sweptback wings of aspect ratios 2 and 3.5. The experimental data, which were obtained in the transonic nozzle of the Langley 9- by 12-inch supersonic blowdown tunnel, indicated that a given wing at a given Mach number fluttered at essentially a fixed dynamic pressure regardless of the individual values of the fluid velocity and density. In contrast to the experimental results, the analytical results which were based on two-dimensional incompressible aerodynamic coefficients indicated that, for the wings tested, the dynamic pressure required for flutter varied with mass ratio.

INTRODUCTION

Flutter theory indicates that fluid velocity and density are distinct variables. For certain groups of wings, however, low-speed flutter investigations (see, for example, refs. 1 and 2) have shown that over a large range of mass ratios (ratio of wing mass to fluid mass) flutter for a given wing occurs at essentially a constant value of the product of the fluid density and the square of the velocity (that is, constant dynamic pressure). Use of the constant-dynamic-pressure flutter concept greatly reduces some of the problems associated with obtaining experimental flutter data and facilitates the correlation of such data.

The use of the dynamic pressure as a defining flutter parameter is particularly advantageous at transonic Mach numbers. The variation with Mach number of dynamic pressure for flutter can be readily obtained in a variable-density wind tunnel with a single model or models of a single design. The dynamic pressure which an airplane encounters in flight is, of course, a function only of altitude and Mach number. Hence, by use of proper scale factors, flutter model results expressed in the form of dynamic pressure as a function of Mach number can be immediately interpreted in terms of the Mach number and altitude at which flutter will occur in flight. If dynamic pressure cannot be used as a defining parameter, however, the investigator must resort to tests of many different models designed to simulate various combinations of altitudes and reduced velocities at each Mach number. Many of the recent transonic flutter investigations have tacitly assumed that dynamic pressure can be used as a defining parameter. Available data tend to justify this assumption; however, the data are limited to a relatively small range of mass ratios.

Transonic flutter studies covering a large range of mass ratios have been made in the transonic nozzle of the Langley 9- by 12-inch supersonic blowdown tunnel. The data, which were obtained in tests of untapered 45° sweptback wings of aspect ratios 2 and 3.5, are presented herein as an aid in evaluating the validity of employing dynamic pressure as a basic parameter in transonic flutter investigations.

SYMBOLS

A	aspect ratio, $\frac{2l \cos \Lambda}{c_s}$
a	nondimensional elastic-axis position measured normal to the leading edge from midchord, positive rearward, semichords; speed of sound
b	wing semichord normal to leading edge, ft
c	wing chord normal to leading edge, in.
c_s	wing chord parallel to free stream, ft
f	frequency of oscillation, cps
$f_{h,1}$	first-bending natural frequency, cps
$f_{h,2}$	second-bending natural frequency, cps
f_α	first torsional natural frequency, $f_{\alpha,c} = \frac{\omega_{\alpha,c}}{2\pi}$, cps
GJ	torsional stiffness about wing elastic axis, lb-ft^2

I_α mass moment of inertia per unit length of wing about the elastic axis, slug-ft

l length of wing parallel to leading edge, ft

M Mach number

m mass per unit length of wing, slugs/ft

q dynamic pressure, $1/2\rho V^2$, lb/sq ft

r_α nondimensional radius of gyration of wing about elastic axis, $\sqrt{I_\alpha/mb^2}$, fraction semichord

t wing thickness, in.

V free-stream velocity, ft/sec

x_α nondimensional wing-section center-of-gravity location measured normal to the leading edge from elastic axis, positive rearward, fraction semichord

ρ air density, slugs/cu ft

μ mass ratio, $m/\pi\rho b^2$

ω frequency of oscillation, radians/sec

$\omega_{h,1}$ first-bending natural frequency, radians/sec

$\omega_{h,2}$ second-bending natural frequency, radians/sec

ω_α first torsional natural frequency $\left(\text{for a uniform cantilevered beam } \omega_{\alpha,c} = \frac{\pi}{2l}\sqrt{\frac{GJ}{I_\alpha}}\right)$, radians/sec

Λ sweepback angle, deg

Subscripts:

e experimental value at flutter

R calculated value at flutter based on a three-degree-of-freedom analysis of form similar to that of reference 3 m measured

c calculated using uniform cantilever beam theory

MODELS

Plan forms of the cantilever-mounted semispan models used in the present investigation are shown in figure 1. All the wings were untapered and swept back 45°. One series was of aspect ratio 2; the other, of aspect ratio 3.5.

Solid magnesium, aluminum, and steel construction were used to obtain the desired mass variation. In order that flutter could be obtained within the operating range of the tunnel, the wing stiffness was varied by varying the thickness (see fig. 1) of the wing's hexagonal airfoil section. Each wing is designated by two digits and a letter. The first digit denotes the aspect ratio. The letter denotes the type of material (M-magnesium, A-aluminum, S-steel) and the final digit denotes the various wings of a given series.

Physical characteristics of the individual wings are listed in table I. The wing thickness, chord, and mass were measured; the nondimensional radius of gyration was calculated by using the measured geometric and mass characteristics of the models. On the basis of the usual effective root assumptions for swept wings (see ref. 3, for example) and the fore-and-aft symmetry of the hexagonal wing sections, the center of gravity and the elastic axis were assumed to lie along the wing midchord line.

Measured frequencies for the various wings are also listed in table I. Typical experimentally determined node lines presented in figure 2 indicate that, for these low-aspect-ratio wings, the modes corresponding to the two higher frequencies were highly coupled. (Vibration modes of the aspect-ratio-2 wings were identified by reducing the span of the higher-aspect-ratio wing in small decrements and observing the changes in the nodal patterns.) Nevertheless, for simplicity, the measured frequencies are used as uncoupled frequencies in the present report. Measured torsional frequencies for the aspect-ratio-2 wings were found to be highly erratic; therefore, calculated torsional frequencies, based on the elementary beam-theory equation for ω_α given in the section "Symbols" and torsional stiffnesses computed from the data given in table I, were used in the reduction of the experimental flutter data for these wings ($A = 2$) and are listed in table I. It is, of course, recognized that the calculated frequencies are a very poor approximation to the magnitude of the actual frequencies; however, they serve as a satisfactory normalizing factor in the reduction of the test data for the aspect-ratio-2 wing.

TEST FACILITY

All the experimental results reported herein were obtained in the transonic nozzle of the Langley 9- by 12-inch supersonic blowdown tunnel. Top and side walls of the 7-inch-high, 10-inch-wide test section of the nozzle are slotted longitudinally to permit operation at and above sonic speed. The floor of the tunnel serves as a reflection plane from which semispan models are cantilever-mounted.

Control of the tunnel stagnation pressure over the operating range of the nozzle (approximately 16 to 31 pounds per square inch absolute) is accomplished by means of a throttling valve located upstream of the test section. Variable and continuous regulation of the test section Mach number is provided by a cylindrical plunger located in the closed-wall part of the tunnel downstream of the test section. By extending the plunger into the airstream, the tunnel can be choked at any desired Mach number. This arrangement of throttling valve and Mach number control plunger permits independent changes of the Mach number and stagnation pressure. In addition to the throttling valve, a quick-acting butterfly valve is located upstream of the test section to provide rapid shutdown of the tunnel.

Condensation-free flow is assured through the use of air dryers and heaters which are installed upstream of the test section. Tunnel surveys indicate that the maximum deviation of the local Mach number from the test-section average varies from ± 0.005 at $M = 0.75$ to ± 0.020 at $M = 1.25$.

INSTRUMENTATION

A resistance-type, electrical strain gage was installed on the surface of the wing near the root (see fig. 1) to establish the occurrence of flutter and to indicate the frequency of the flutter oscillation. The signal from the strain gage was amplified and fed into a recording oscillograph to obtain a time history of the motion.

In addition to the strain-gage output, simultaneous and continuous measurements of the tunnel static pressure and the stagnation pressure and temperature were recorded by the multichannel oscillograph. At flutter, independent measurements of the pressure (indicated on mercury manometers) were recorded photographically.

TEST PROCEDURE

The test procedure was the same as that of reference 4; flutter points were obtained by approaching the flutter condition by one of two procedures: (1) setting the Mach number control plunger in a desired position and varying the test-section density by increasing the tunnel stagnation pressure in small increments until flutter was obtained or (2) setting the tunnel stagnation pressure at a desired value and increasing (or decreasing) the Mach number in small increments until the model fluttered. In many instances it was found convenient to vary alternately both the Mach number and stagnation pressure during the course of obtaining a flutter point.

RESULTS AND DISCUSSION

Experimental Data

Results of the experimental investigation are listed in table II. (In some cases, as denoted by the blanks in the table, the flutter frequency could not be determined because of the rapid destruction of the model.) Data from the table have been used in the preparation of figure 3 which shows the variation with Mach number of the flutter-speed coefficient $\frac{V_e}{b\omega_\alpha}$ divided by the square root of the mass ratio μ. The data of figure 3, which were obtained for widely different mass ratios, are seen to fall into a band within which no systematic effects of mass ratio are evident. (It will be shown in the following paragraph that the parameter $\frac{V_e}{b\omega_\alpha \sqrt{\mu}}$ (or the companion parameter $\frac{b\omega_\alpha}{a}\sqrt{\mu}$, a form used in many recent flutter reports) serves as a satisfactory correlating factor only if flutter at a given Mach number occurs at fixed dynamic pressure.) The small variation of $\frac{V_e}{b\omega_\alpha \sqrt{\mu}}$ with Mach number exhibited by the data appear to be consistent with the trends indicated by the data of references 5 and 6.

In order to illustrate the effects of mass ratio on flutter better, the data have been replotted in figure 4 as the variation of the flutter-speed coefficient with the square root of the mass ratio for small increments in Mach number. (Effects of Mach number over the small increments (see fig. 3) are negligible.) As shown in figure 4 the flutter-speed coefficients vary almost linearly with the square root of the mass ratio and can be approximated by straight lines which, if extended, would as shown by the dotted lines pass through the origins. Therefore the effect of both μ and $\frac{V_e}{b\omega_\alpha}$ can be expressed in terms of a single parameter $\frac{V_e}{b\omega_\alpha \sqrt{\mu}}$, the slope of the lines. By using the relations for μ, ω_α, r_α, and q found in the section entitled "Symbols," it can be shown that the square of this parameter is proportional to q:

$$\left(\frac{V_e}{b\omega_\alpha\sqrt{\mu}}\right)^2 = q\left(\frac{8l^2b^2{r_\alpha}^2}{\pi GJ}\right)$$

The terms enclosed in parentheses on the right-hand side of the equation are functions of the wing geometry and structure only. Therefore the straight lines of figure 4 indicate that, for the range of variables tested, flutter for a given wing at any given Mach number occurs at essentially a fixed dynamic pressure, regardless of the individual values of fluid velocity and density.

Analytical Results

Two-dimensional incompressible aerodynamic coefficients were used in an analysis similar to that of reference 3 to determine the flutter-speed characteristics of untapered 45° sweptback wings of aspect ratios 2, 3.5, and ∞. In the analysis, the flutter mode was represented by the superposition of the first and second bending and first torsion mode shapes of a uniform cantilever beam. The more important parameters used in these calculations are of the same order of magnitude as the experimental values listed in table I and are as follows:

Aspect ratio	a or x_α	${r_\alpha}^2$	$(\omega_{h,1}/\omega_\alpha)^2$	$(\omega_{h,2}/\omega_\alpha)^2$	$m/\pi b^2$	ρ
2	0	0.25	0.021	0.29	0.132	Variable
3.5	0	.25	.013	.40	.422	Variable
∞	0	.25	.015	.35	.500	Variable

The results of the calculations are presented in figure 5 in the form of flutter-speed coefficient as a function of the square root of the mass ratio. The results for the wing of infinite aspect ratio indicate a linear variation of $V_R/b\omega_\alpha$ with $\sqrt{\mu}$ for all values of $\sqrt{\mu}$ above about 2. Extrapolation of the linear portion of the curve for this wing to a zero value of $\sqrt{\mu}$ indicates only a small intercept on the axis of $V_R/b\omega_\alpha$. Thus, for this case, the analytical results indicate flutter to occur at a nearly constant value of the dynamic pressure. This result is consistent with trends shown in reference 2 for unswept wings of various aspect ratios. The curve for the swept wing of aspect ratio 3.5 and the lower curve for the swept wing of aspect ratio 2 follow the same general trend as shown by the wing of infinite aspect ratio at the low and intermediate values of $\sqrt{\mu}$. For the higher mass ratios, however, the curves for the wings of finite aspect ratio indicate a change in slope of the curve of the variation of $V_R/b\omega_\alpha$ with $\sqrt{\mu}$. Thus, the analytical method does not predict even approximately a fixed dynamic-pressure flutter for the finite aspect ratio wings over this mass-ratio range. As an example, for the aspect-ratio-2 wing the analytical method predicts approximately a 55-percent decrease in q as the square root of the mass ratio is increased from 7.0 to 12.5 (the mass-ratio range covered by the experimental data for $0.91 < M_e < 0.98$). The variation is somewhat less for the aspect-ratio-3.5 wings.

From a study of the flutter equations it was noted that the terms which produced the large decrease in the dynamic pressure required for flutter indicated by the calculated curves at the higher mass ratios involved the parameter $\frac{\tan \Lambda}{l/b}$ as a multiplier. Therefore, as indicated by the data of figure 5 and reference 2, the large decreases in dynamic pressure shown for the wings of aspect ratio 2 and 3.5 would not be expected for swept wings of high aspect ratio or unswept wings of any aspect ratio.

In order to correlate data obtained under varying test conditions, the results of many recent flutter investigations (see, for example, refs. 4 to 6) have been presented as the ratio of the experimental to the calculated flutter speed. The results of the present investigation indicate that caution should be exercised in the use and interpretation of this form of data presentation for low-aspect-ratio sweptback wings at high mass ratios. For example, the results of the present investigation correlated on the basis of flutter-speed ratio indicate an independent effect of mass ratio on the flutter-speed ratio, whereas the experimental data indicate that the flutter speed varies linearly with the square root of the mass ratio.

It is interesting to note that for the wings of aspect ratio 2 and 3.5 at high mass ratios a second noncritical root of the flutter equation is encountered. (The second root for the aspect-ratio-3.5 wing is encountered at flutter-speed coefficients greater than 15 and is not shown in fig. 4.) Although the second root occurs at a higher flutter-speed coefficient, at some mass ratios it occurs at a lower value of the reduced velocity $\left(\frac{V}{b\omega}\right)_R$ than that of the critical root. It was found that the second root stems from the zero airspeed torsional mode of vibration, whereas the critical root emanates from the second bending mode at the lower mass ratios and the first bending mode at the higher mass ratios.

CONCLUSIONS

The following conclusions were reached as a result of a study of the effects of mass ratio on the transonic flutter characteristics of untapered 45° sweptback wings of aspect ratios 2 and 3.5:

1. The experimental data indicate that, for the range of variables tested, a given wing at a given Mach number fluttered at essentially a fixed dynamic pressure regardless of the individual values of fluid velocity and density.

2. In contrast to the experimental results, the analytical results which were based on two-dimensional incompressible aerodynamic coefficients indicated that, for the wings tested, the dynamic pressure required for flutter varied with mass ratio.

Langley Aeronautical Laboratory,
National Advisory Committee for Aeronautics,
Langley Field, Va., March 28, 1958.

REFERENCES

1. Theodorsen, Theodore, and Garrick, I. E.: Mechanism of Flutter - A Theoretical and Experimental Investigation of the Flutter Problem. NACA Rep. 685, 1940.

2. Woolston, Donald S., and Castile, George E.: Some Effects of Variations in Several Parameters Including Fluid Density on the Flutter Speed of Light Uniform Cantilever Wings. NACA TN 2558, 1951.

3. Barmby, J. G., Cunningham, H. J., and Garrick, I. E.: Study of Effects of Sweep on the Flutter of Cantilever Wings. NACA Rep. 1014, 1951. (Supersedes NACA TN 2121.)

4. Pratt, George L.: Experimental Flutter Investigation of a Thin Unswept Wing at Transonic Speeds. NACA RM L55A18, 1955.

5. Jones, George W., Jr., and Unangst, John R.: Investigation To Determine Effects of Center-of-Gravity Location on Transonic Flutter Characteristics of a 45° Sweptback Wing. NACA RM L55K30, 1956.

6. Ruhlin, Charles L.: Experimental Transonic Flutter Characteristics of an Untapered, 45° Sweptback, Aspect-Ratio-4 Wing. NACA RM L55L22, 1956.

TABLE I.- PHYSICAL CHARACTERISTICS OF THE INDIVIDUAL WINGS

$[a = 0;\ x_\alpha = 0.]$

Wing	t, in.	c, in.	m, slugs/ft	r_α^2	$f_{h,1,m}$, cps	$f_{h,2,m}$, cps	$f_{\alpha,m}$, cps	$\omega_{h,1,m}/\omega_{\alpha,m}$	$\omega_{h,2,m}/\omega_{\alpha,m}$	$f_{\alpha,c}$, cps
Aspect ratio 2										
2-S-1	0.020	1.420	0.00270	0.248	73	290	510	0.143	0.569	356
2-S-2	.018	1.414	.00225	.248	75	237	500	.150	.474	323
2-S-3	.018	1.414	.00225	.248	75	237	500	.150	.474	323
2-S-4	.020	1.421	.00273	.247	79	330	585	.135	.564	342
2-S-5	.019	1.416	.00265	.249	80	242	540	.147	.449	339
2-S-6	.020	1.414	.00270	.248	81	320	582	.139	.550	355
2-S-7	.022	1.418	.00309	.248	91	345	642	.142	.537	389
2-S-8	.019	1.416	.00265	.249	72	276	497	.146	.555	339
2-S-9	.020	1.420	.00270	.248	82	273	586	.139	.466	356
2-S-10	.020	1.417	.00270	.248	75	290	540	.139	.537	346
2-S-11	.023	1.422	.00312	.247	91	298	600	.152	.497	393
2-A-1	.031	1.410	.00120	.248	139	525	975	.143	.538	534
2-A-2	.031	1.400	.00141	.250	130	487	950	.137	.513	533
2-A-3	.032	1.422	.00146	.248	124	484	925	.134	.524	535
2-A-4	.031	1.400	.00141	.250	125	500	865	.144	.578	533
2-A-5	.031	1.410	.00120	.248	125	485	900	.139	.539	534
2-A-6	.031	1.416	.00146	.248	124	472	873	.142	.541	524
2-A-7	.031	1.410	.00120	.248	122	498	850	.144	.586	534
2-A-8	.031	1.418	.00146	.248	138	510	943	.146	.541	524
2-A-9	.031	1.410	.00120	.248	139	525	975	.143	.538	534
2-A-10	.031	1.408	.00133	.258	100	418	900	.111	.464	554
2-M-1	.030	1.421	.00095	.247	123	550	910	.135	.605	508
2-M-2	.033	1.412	.00095	.248	127	605	920	.138	.658	576
2-M-3	.032	1.414	.00093	.249	111	470	732	.152	.642	555
2-M-4	.033	1.412	.00095	.248	145	540	970	.150	.557	576
2-M-5	.030	1.420	.00094	.248	116	565	732	.130	.635	499
2-M-6	.032	1.414	.00093	.249	111	470	970	.152	.642	555
2-M-7	.033	1.412	.00095	.248	145	540	970	.150	.557	576
2-M-8	.032	1.421	.00098	.247	93	435	778	.120	.559	528
2-M-9	.030	1.421	.00095	.247	120	460	808	.149	.569	508
2-M-10	.033	1.412	.00095	.248	129	505	862	.150	.586	576
2-M-11	.032	1.421	.00097	.248	112	508	850	.132	.598	529
2-M-12	.033	1.412	.00095	.248	145	540	925	.150	.557	576
2-M-13	.032	1.421	.00098	.247	134	605	890	.145	.654	528
Aspect ratio 3.5										
3.5-S-1	0.038	1.417	0.00510	0.249	48	258	400	0.120	0.645	
3.5-S-2	.036	1.414	.00457	.250	44	245	388	.115	.631	
3.5-S-3	.036	1.416	.00460	.250	45	246	389	.116	.632	
3.5-S-4	.038	1.415	.00504	.248	48	262	402	.118	.651	
3.5-S-5	.036	1.413	.00461	.251	45	245	388	.116	.631	
3.5-S-6	.036	1.414	.00466	.250	44	248	385	.116	.644	
3.5-S-7	.038	1.409	.00501	.249	49	259	415	.118	.624	
3.5-S-8	.036	1.413	.00457	.251	44	240	384	.115	.624	
3.5-S-9	.038	1.415	.00508	.248	50	261	412	.120	.633	
3.5-A-1	.052	1.416	.00236	.248	65	345	552	.118	.624	
3.5-A-2	.051	1.415	.00235	.252	63	352	545	.116	.646	
3.5-A-3	.051	1.413	.00229	.253	67	368	555	.121	.663	
3.5-A-4	.051	1.407	.00229	.254	66	366	550	.120	.665	
3.5-A-5	.052	1.414	.00236	.249	67	340	551	.122	.617	
3.5-A-6	.051	1.415	.00234	.252	67	358	552	.121	.649	
3.5-A-7	.052	1.408	.00224	.249	71	380	570	.125	.666	
3.5-A-8	.051	1.413	.00233	.253	66	354	546	.121	.648	

[redacted]

TABLE II.- EXPERIMENTAL FLUTTER CHARACTERISTICS

Wing	M_e	q_e, lb/ft^2	μ_e	V_e, ft/sec	f_e, cps	$\frac{V_e}{b\omega_{\alpha,c}}$	$\frac{\omega_e}{\omega_{\alpha,c}}$	$\frac{V_e}{b\omega_e}$
Aspect ratio 2								
2-S-1	0.772	1,063	81.2	830	217	6.271	0.610	10.280
2-S-2	.790	833	95.7	880	188	7.355	.582	12.637
2-S-3	.799	778	106.6	890	187	7.438	.579	12.846
2-S-4	.896	1,111	111.0	999	190	7.851	.556	14.120
2-S-5	.922	914	135.5	1,012	---	8.060	-----	------
2-S-6	.945	981	152.7	1,099	180	8.370	.507	16.509
2-S-7	.961	1,506	94.3	1,080	200	7.474	.514	14.541
2-S-8	.971	979	147.1	1,091	184	8.690	.543	16.004
2-S-9	1.030	1,046	154.1	1,145	175	8.651	.492	17.583
2-S-10	1.104	1,239	150.4	1,231	180	9.580	.520	16.423
2-S-11	1.168	1,713	122.0	1,216	214	8.317	.544	15.289
2-A-1	.889	1,157	48.1	1,001	272	5.082	.509	9.984
2-A-2	.913	1,471	46.9	1,023	300	5.233	.563	9.295
2-A-3	.949	1,340	51.6	1,023	290	5.138	.542	9.480
2-A-4	1.019	1,216	65.3	1,097	258	5.611	.484	11.593
2-A-5	1.050	1,396	51.7	1,140	288	5.788	.539	10.738
2-A-6	1.091	1,378	64.1	1,153	274	5.932	.523	11.342
2-A-7	1.097	1,628	46.8	1,172	---	5.951	-----	------
2-A-8	1.156	1,567	66.7	1,254	300	6.452	.572	11.280
2-A-9	1.180	1,256	67.8	1,239	255	6.291	.478	13.161
2-A-10	1.248	1,615	64.0	1,302	300	6.370	.542	11.753
2-M-1	.719	920	30.9	808	332	4.272	.654	6.532
2-M-2	.739	944	30.7	826	324	3.835	.562	6.824
2-M-3	.791	1,008	34.7	907	325	4.411	.586	7.527
2-M-4	.813	1,189	31.2	923	---	4.338	-----	------
2-M-5	.828	846	47.4	966	300	5.208	.601	8.666
2-M-6	.829	926	39.7	919	323	4.470	.564	7.926
2-M-8	.835	995	37.0	920	320	4,324	.556	7.777
2-M-8	.870	811	55.2	1,003	300	5.107	.568	8.991
2-M-9	.896	863	53.8	1,033	275	5.461	.541	10.094
2-M-10	.934	1,048	47.5	1,070	300	5.029	.521	9.652
2-M-11	.945	914	58.0	1,098	290	5.576	.548	10.175
2-M-12	.950	966	52.3	1,077	---	5.062	-----	------
2-M-13	1.075	1,062	54.7	1,143	293	5.820	.555	10.486
Aspect ratio 3.5								
3.5-S-1	0.930	1,399	164.5	994	---	6.704	-----	------
3.5-S-2	.966	1,082	238.9	1,111	---	7.737	-----	------
3.5-S-3	.996	1,020	264.8	1,133	---	7.857	-----	------
3.5-S-4	1.017	1,283	205.5	1,070	125	7.180	0.311	23.087
3.5-S-5	1.032	1,051	271.5	1,162	---	8.092	-----	------
3.5-S-6	1.057	1,065	284.1	1,191	116	8.359	.301	27.771
3.5-S-7	1.079	1,205	244.4	1,129	115	7.376	.277	26.628
3.5-S-8	1.220	1,274	285.1	1,315	---	9.253	-----	------
3.5-S-9	1.231	1,591	227.5	1.249	141	8.178	.342	23.912
3.5-A-1	.827	1,376	62.1	890	203	4.349	.368	11.818
3.5-A-2	.878	1,300	80.2	985	194	4.879	.356	13.705
3.5-A-3	.929	901	133.2	1,066	160	5.190	.288	18.021
3.5-A-3	.945	914	134.7	1,080	160	5.258	.268	18.257
3.5-A-4	.947	1,265	92.9	1,053	188	5.211	.342	15.237
3.5-A-4	.969	1,071	117.3	1,089	172	5.375	.313	17.172
3.5-A-4	.975	997	128.2	1,098	167	5.420	.304	17.829
3.5-A-5	.976	949	131.9	1,077	152	5.281	.276	19.134
3.5-A-6	.979	966	139.0	1.145	162	5.595	.294	19.031
3.5-A-7	.998	1,086	112.8	1,088	---	5.178	-----	------
3.5-A-8	1.078	1,110	135.6	1,186	160	5.869	.293	20.031
3.5-A-8	1.198	1,214	148.3	1,297	175	6.419	.322	19.935

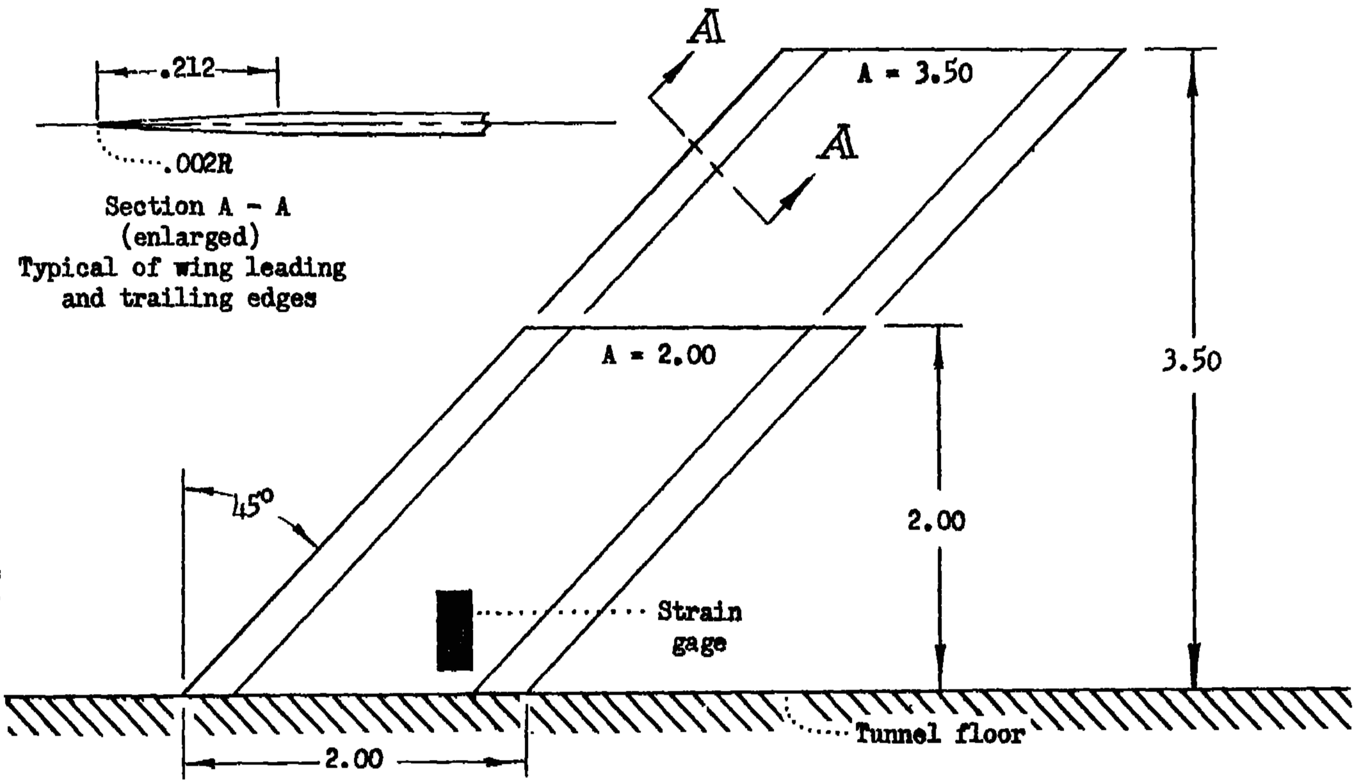

Aspect ratio	2.00			3.50	
Wing	2-S	2-A	2-M	3.5-S	3.5-A
Material	Steel	Aluminum	Magnesium	Steel	Aluminum
Thickness ratio (Streamwise)	.010	.016	.016	.018	.025

Figure 1.- Layout of wings. (Linear dimensions are in inches.)

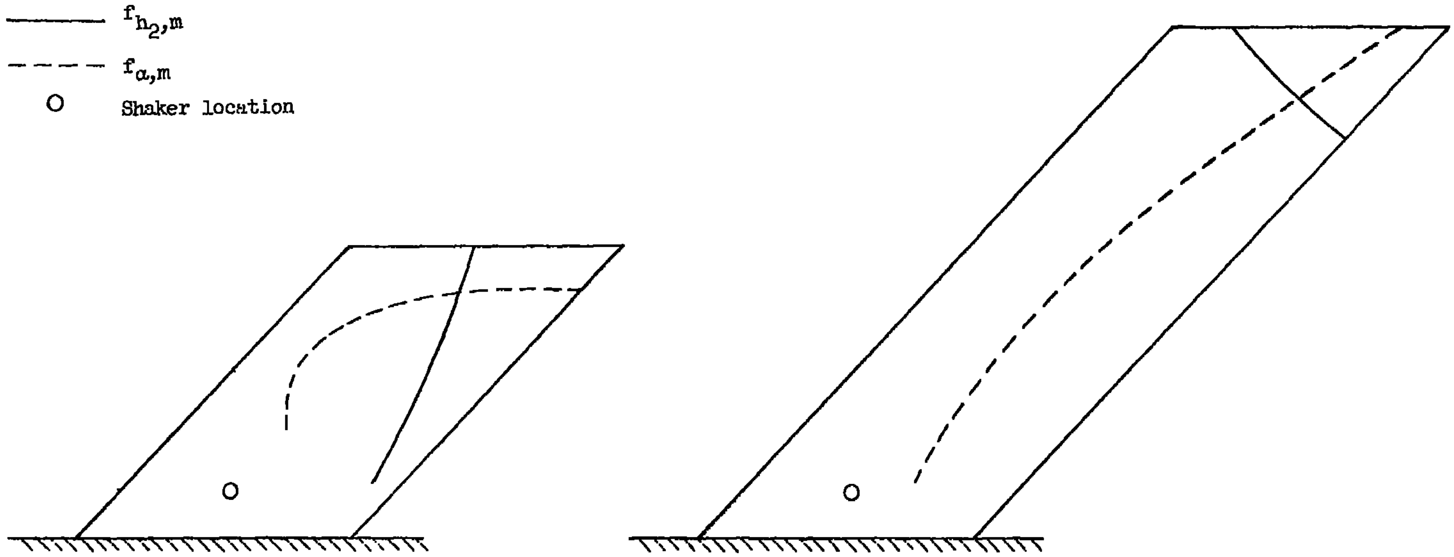

(a) Aspect ratio 2.0.

(b) Aspect ratio 3.5.

Figure 2.- Typical experimental node lines.

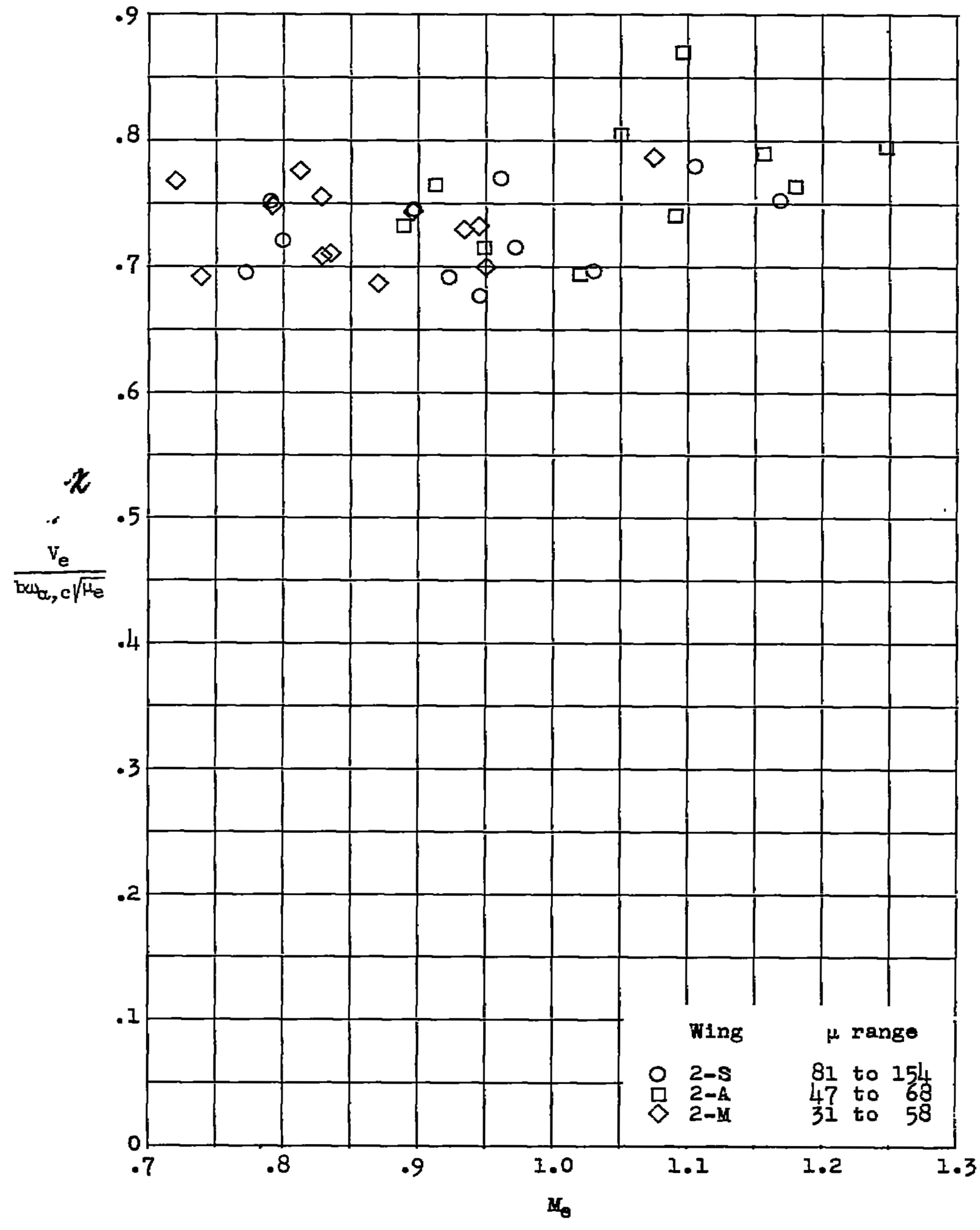

(a) Aspect-ratio-2 wings.

Figure 3.- Experimental variation of $\frac{V_e}{b\omega_\alpha\sqrt{\mu_e}}$ with Mach number.

[redacted]

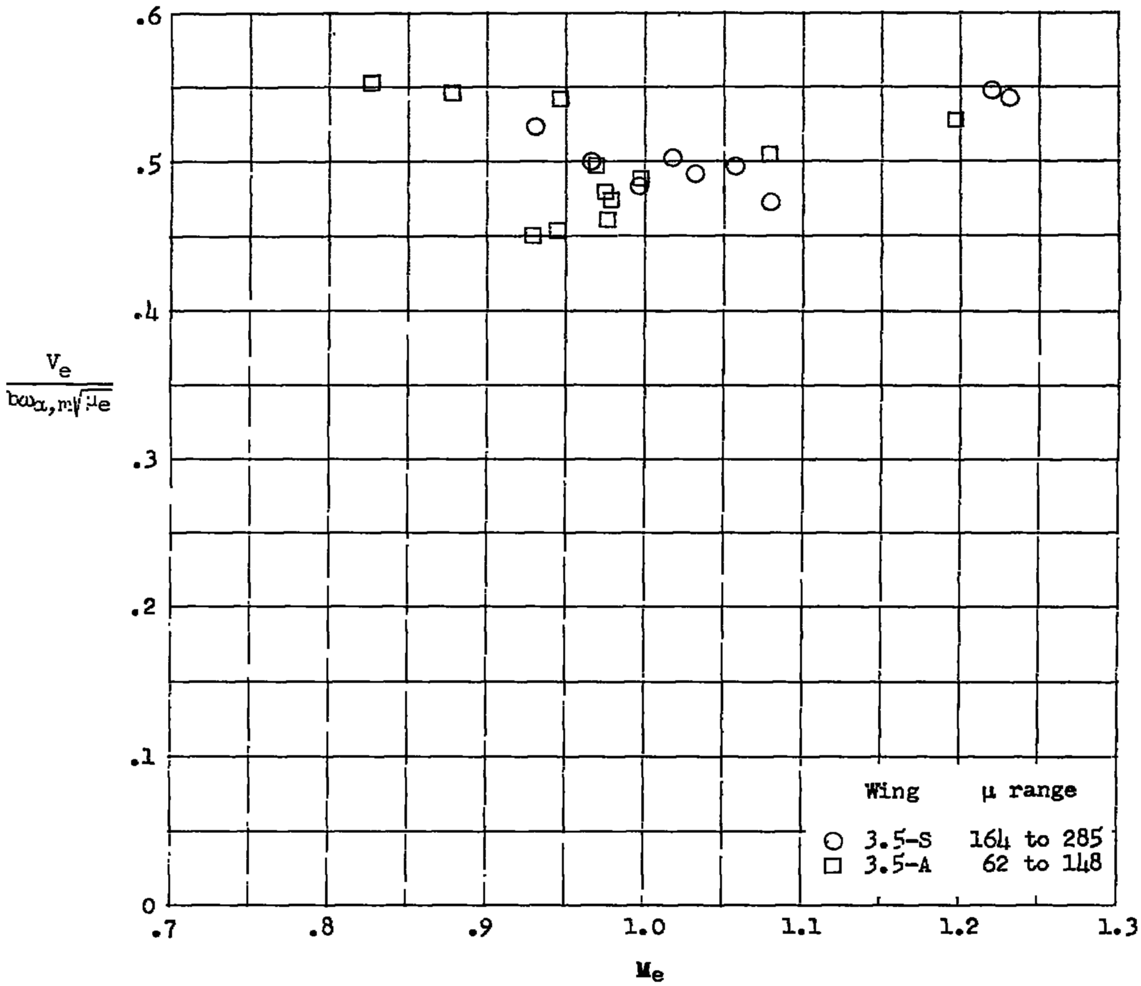

(b) Aspect-ratio-3.5 wings.

Figure 3.- Concluded.

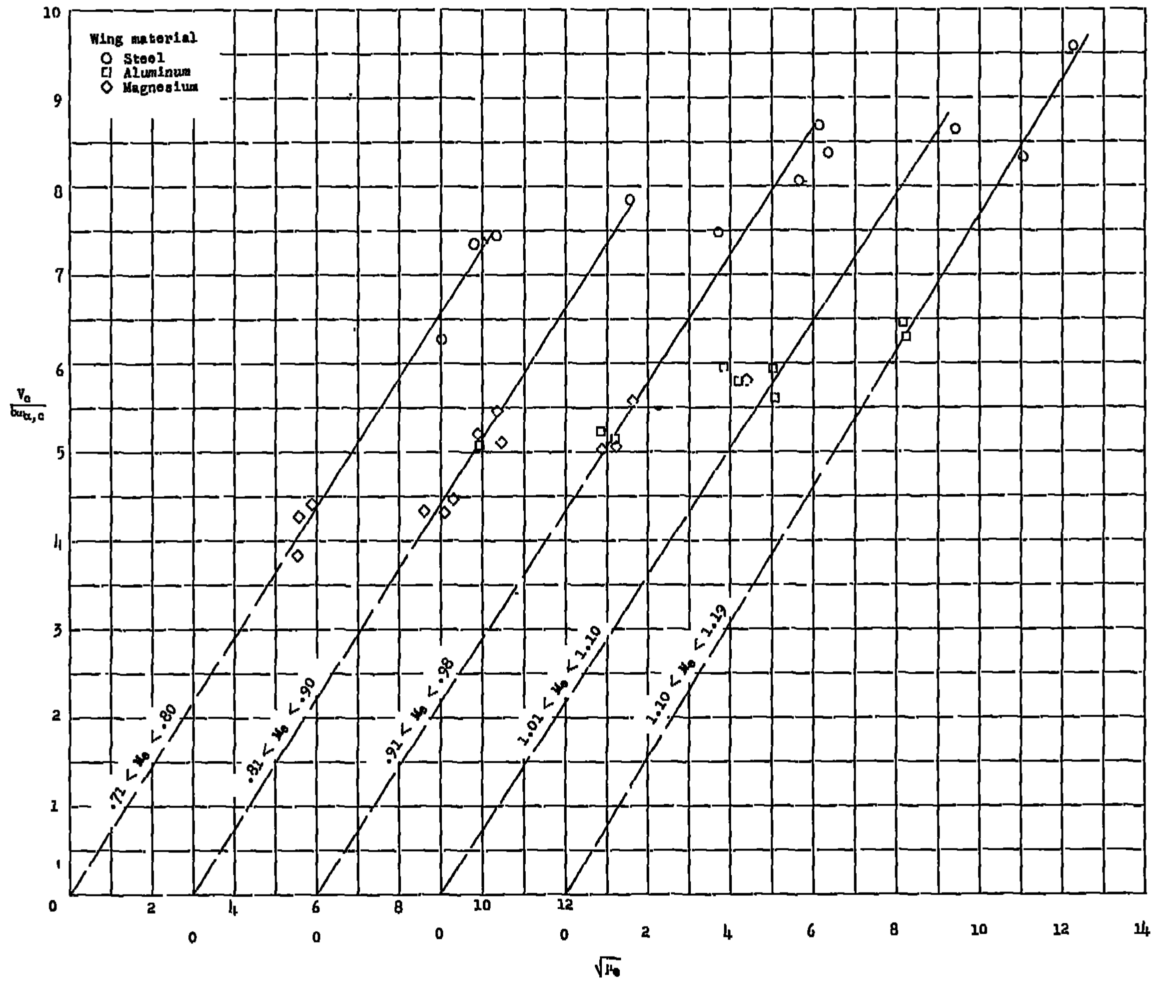

(a) Aspect-ratio-2 wings.

Figure 4.- Variation of the experimental flutter-speed coefficients with the square root of the mass ratio for small increments in Mach number.

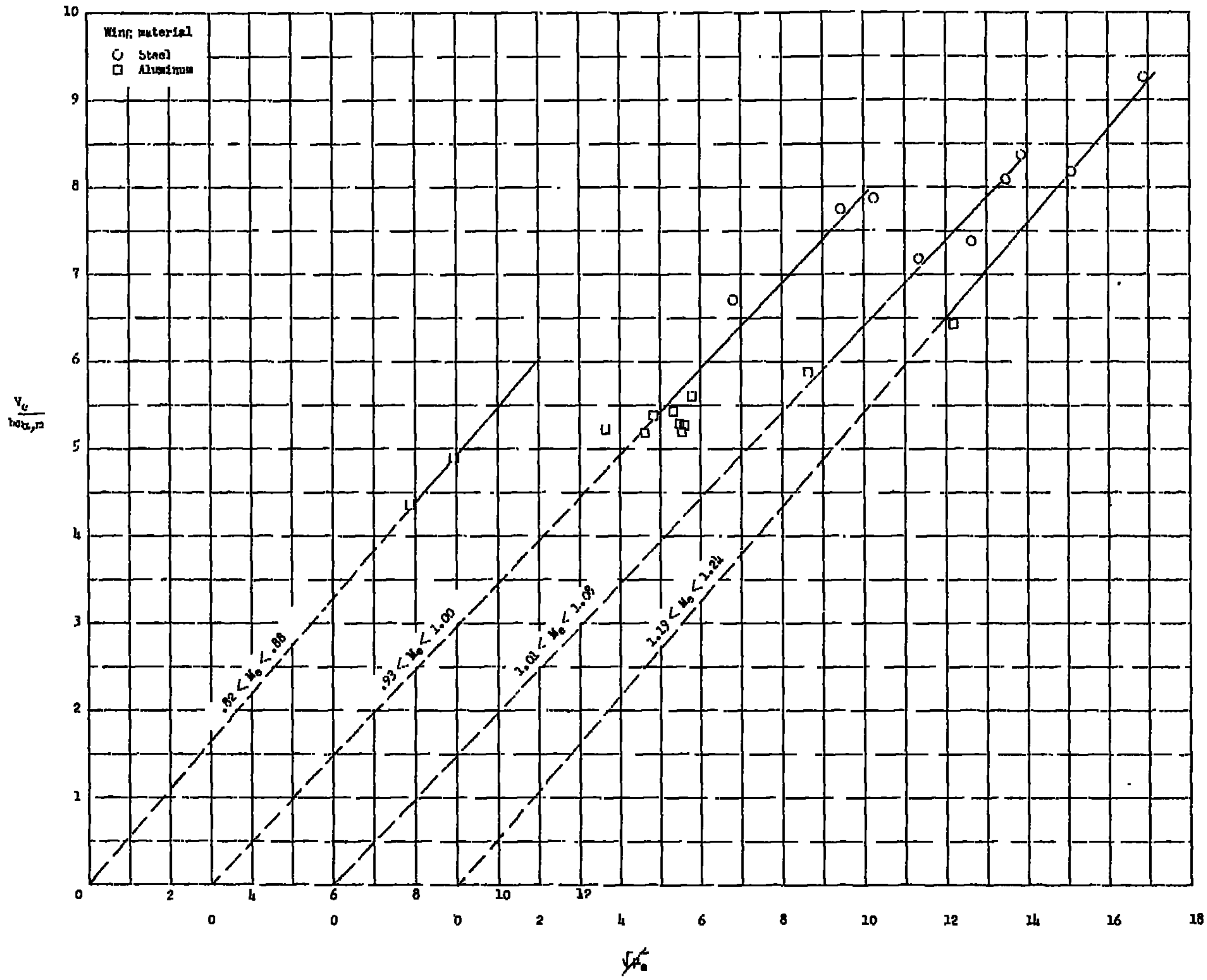

(b) Aspect-ratio-3.5 wings.

Figure 4.- Concluded.

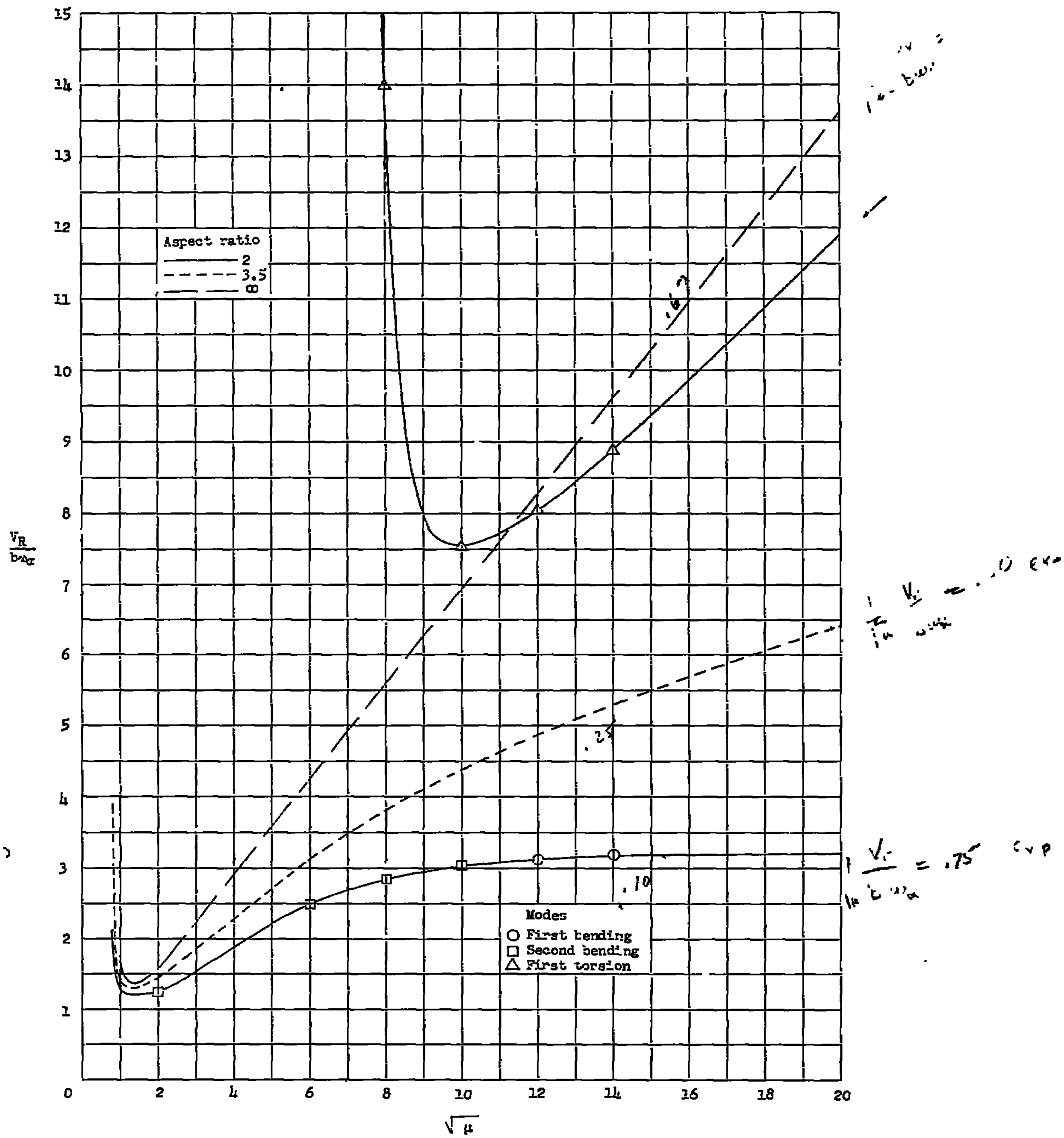

Figure 5.- Variation of the calculated flutter-speed coefficient with the square root of the mass ratio. Symbols denote fundamental mode from which flutter stems.

[redacted]